

## Synthesis and Properties of 2,3-Dialkynyl-1,4-benzoquinones

Peter Hammershøj,<sup>[a]</sup> Theis K. Reenberg,<sup>[a]</sup> Michael Pittelkow,<sup>[a]</sup> Christian B. Nielsen,<sup>[a]</sup> Ole Hammerich,<sup>[a]</sup> and Jørn B. Christensen\*<sup>[a]</sup>

**Keywords:** Benzoquinones / Acetylenes / Sonogashira cross-coupling / Cyclic voltammetry / UV/Vis / DFT calculations

Alkynyl substituents can be used to tune the acceptor properties of benzoquinones due to their slight electron-withdrawing abilities. Applications of new acceptors rely on efficient and practical synthetic procedures. Herein we describe a general and convenient approach for the synthesis of 2,3-dialkynyl-1,4-benzoquinones using a combination of regioselective aromatic substitution, Sonogashira cross-couplings and mild CAN oxidation chemistry. The regiochemical

outcome of the synthetic protocol was verified by X-ray crystallography of two compounds. Cyclic voltammetry, UV/Vis and DFT calculations on three derivatives show that the symmetrical dialkynyl-substituted benzoquinones are attractive acceptors.

(© Wiley-VCH Verlag GmbH & Co. KGaA, 69451 Weinheim, Germany, 2006)

### Introduction

The design and synthesis of components for organic electronics is important for many areas of materials science such as non-linear optics, electronic transistors, molecular switches and chemical sensors. Transportation of charge is important in materials science, where the vast majority of organic conducting materials are hole-conductors based on radical cationic states of organic molecular crystals or polymers. Simple quinones such as benzoquinone, chloranil or DDQ have been used as acceptors in charge-transfer complexes,<sup>[1]</sup> and recently the first example of a metallic CT complex with chloranil was reported.<sup>[2]</sup> Quinones are also widespread in nature having functions involving electron- and proton-transport. Important biological quinones covers a wide range of structure from Ubiquinone via Vitamin K to pyrroloquinoline quinone (Figure 1).<sup>[3–5]</sup>

Quinones can in general be viewed as two carbonyl groups connected (in conjugation) via a  $\pi$ -framework and the electronic properties should therefore be tunable by changing the pathway of conjugation. The simplest example of this is *ortho*- and *para*-benzoquinones, but a change in the conjugated pathway can also be achieved by the two different naphthoquinones in Figure 2. A simple way to introduce diversity is by varying the regiochemistry as illustrated by the three different dialkynyl-substituted 1,4-benzoquinones.

Our interest in 2,3-alkynylated 1,4-benzoquinones originates from a number of fundamental questions. What effect

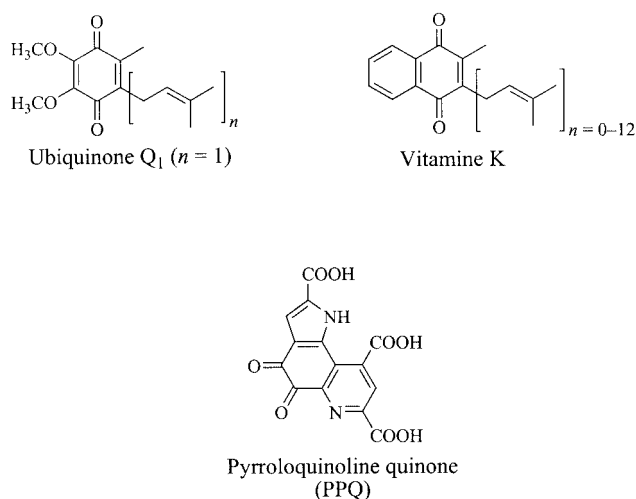


Figure 1. Diverse structures of three naturally occurring quinones.

does cross-conjugation with alkynes have on the acceptor-properties of a quinone? Can 2,3-bis-alkynylated 1,4-benzoquinones serve as building blocks for molecular devices and for larger polycyclic aromatic hydrocarbons? Finally, 1,2,3,4-tetrasubstituted benzenes are relatively rare, and a general practical synthetic protocol for 2,3-dialkynyl-substituted was the first challenge.

A few 2,3-dialkynyl-5,6-disubstituted-1,4-benzoquinones were reported by Komatsu,<sup>[6]</sup> Nicolaou<sup>[7]</sup> and Moore<sup>[8]</sup> but little has been described with respect to the effect of alkynyl substitution. From a study of alkynylated flavins<sup>[9]</sup> as well as from the Hammett  $\sigma$ -parameters it was expected that alkynes would act as electron-withdrawing substituents.<sup>[10]</sup> This has also been shown by the work of Diederich and collaborators on acetylene scaffolding.<sup>[11–13]</sup>

[a] Department of Chemistry, University of Copenhagen, Universitetsparken 5, 2100 Copenhagen Ø, Denmark  
E-mail: jbc@kiku.dk

Supporting information for this article is available on the WWW under <http://www.eurjoc.org> or from the author.

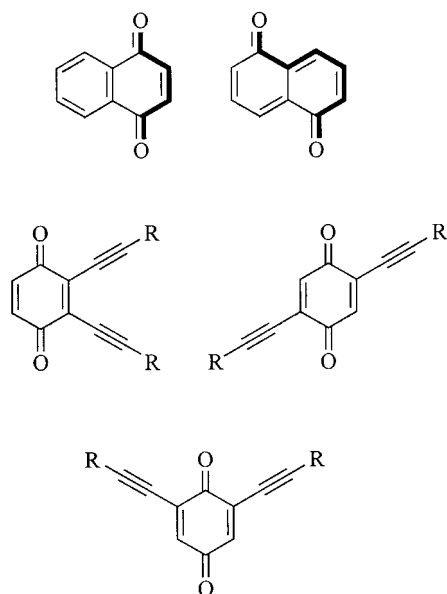


Figure 2. 1,4-Naphthoquinone, 1,5-naphthoquinone and the three different dialkynyl-substituted benzoquinones.

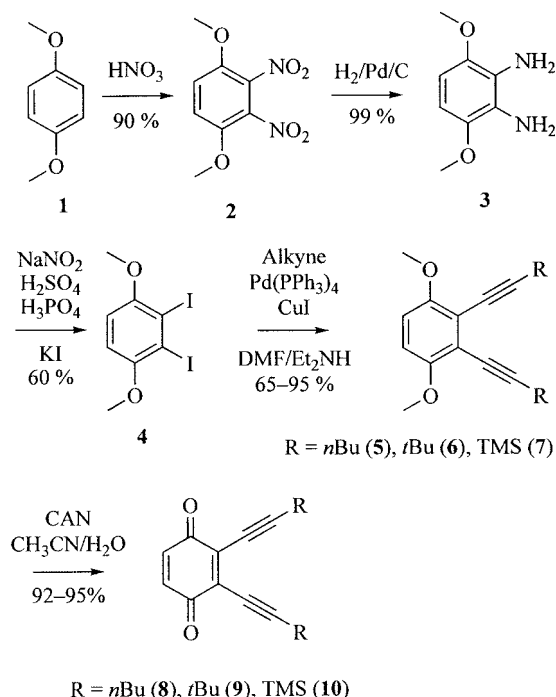
Herein we present a general and convenient protocol for the synthesis of 2,3-dialkynyl-1,4-benzoquinones and a study of their electrochemical and optical properties. A brief computational study using density functional theory (DFT) was undertaken to support the findings from the characterization experiments. Finally, we present two crystal structures that confirm the regiochemistry of the synthetic protocol.

## Results and Discussion

### Synthesis

The synthesis is shown in Scheme 1. Dinitration of 1,4-dimethoxybenzene gave 2,3-dinitro-1,4-dimethoxybenzene (**2**) in 90% isolated yield.<sup>[14,15]</sup> Catalytic hydrogenation with H<sub>2</sub> and Pd/C afforded the diamine **3** in quantitative yield.<sup>[16]</sup> Tetrazotization and subsequent Sandmeyer reaction gave 1,4-dimethoxy-2,3-diiodobenzene (**4**) in 60% yield. We found that careful control of temperature and rate of addition was important for reproducible results.<sup>[17–20]</sup>

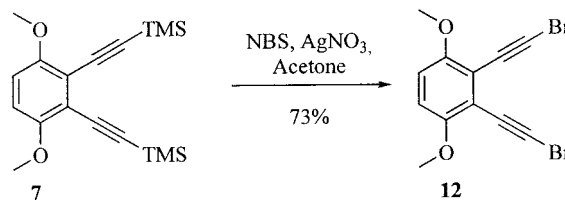
Sonogashira cross-coupling chemistry was unsuccessful under standard thermal conditions when the diiodide **4** was used as the Ar–X component, but by using the procedure of Erdélyi and Gogoll<sup>[21]</sup> it was possible to perform the Sonogashira cross-coupling reaction between terminal alkynes and the diiodide **4** using microwave irradiation. The 1,4-dimethoxy-2,3-dialkynylbenzenes **5–7** were isolated as pale yellow low melting solids after column chromatography on silica. Using these conditions we only observed trace amounts of the mono-substituted adducts. CAN oxidation of the 1,4-dimethoxy functionalities was carried out at room temperature in aqueous acetonitrile to produce the benzoquinones **8–10**.<sup>[22,23]</sup> Diiodide **4** was also oxidized



Scheme 1. The reaction scheme for the synthesis of 2,3-alkynyl-1,4-benzoquinones.

with CAN to the corresponding 2,3-diiodo-1,4-benzoquinone (**11**) in good yield.

1-Haloalkynes can be useful for cross-coupling reactions.<sup>[24,25]</sup> The conversion of the TMS-protected alkyne **7** to the corresponding 1-bromoalkyne was achieved by reaction with NBS and silver nitrate. The resulting dibromoalkyne **12** turned out to be surprisingly stable. The structure was confirmed by X-ray crystallography (Scheme 2).



Scheme 2. Synthesis of the bis(1-bromoalkyne) **12**.

### X-ray Crystallographic Analysis

Both the TMS (**7**) and the bromo (**12**) acetylene analogs were analyzed by single-crystal X-ray crystallography which confirmed the regiochemistry of the synthetic route (Figure 3). Crystals suitable for X-ray analysis of **7** were grown by slow evaporation of a saturated ethyl acetate/*n*-heptane solution and crystals suitable for X-ray analysis of **12** were prepared by slow evaporation of a CH<sub>2</sub>Cl<sub>2</sub> solution.

The TMS acetylene analog **7** crystallizes in the monoclinic space group *P*2<sub>1</sub>/*n* with two molecules in the asymmetric unit and bromide acetylene analog **12** crystallizes in

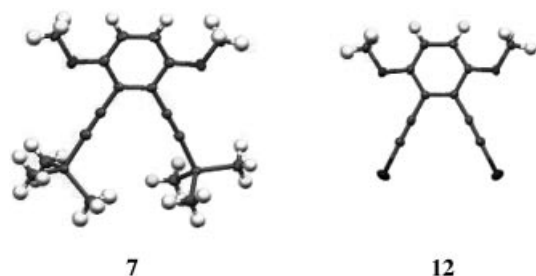


Figure 3. View of molecular structures determined by single-crystal X-ray crystallography of **7** and **12** respectively. The displacement ellipsoids are drawn at the 50% probability level.

the monoclinic space group  $P2_1/c$  with two molecules in the asymmetric unit (Table 1). The bond lengths and angles of the two compounds are comparable to each other and are generally within the normal ranges.

Table 1. Selected crystallographic data of **7** and **12**.

Compound	<b>12</b>	<b>7</b>
Formula	$C_{12}H_8Br_2O_2$	$C_{18}H_{26}O_2Si_2$
Formula mass	344.00	330.57
Crystal system	monoclinic	monoclinic
Space group	$P2_1/c$	$P2_1/n$
Z	8	8
a [Å]	11.601(3)	9.8020(16)
b [Å]	11.624(5)	10.3030(16)
c [Å]	18.658(4)	39.938(6)
$\alpha$	90	90
$\beta$	80.462(14)	90.402(14)
$\gamma$	90	90
V [Å <sup>3</sup> ]	2481.2(12)	4033.2(11)
$\rho$ [g·cm <sup>-3</sup> ]	1.842	1.089
Crystal dimensions [mm]	$0.57 \times 0.10 \times 0.04$	$0.43 \times 0.20 \times 0.09$
Type of radiation	Mo- $K_\alpha$	Mo- $K_\alpha$
$\mu$ [mm <sup>-1</sup> ]	6.515	0.180
T [K]	122(2)	122(2)
No. of reflections	65914	64616
Unique reflections (with $I > 2\sigma$ )	4580	5504
$R_{int}$	0.1228	0.0852
$\Delta\rho_{max}/\Delta\rho_{min}$ [ $e \cdot \text{Å}^{-3}$ ]	1.473/−1.174	0.306/−0.326
$R(F)$ , $R_w(F_2)$ (all data)	0.0513/0.1409	0.0456/0.1187

In both structures the methyl part of the methoxy substituents are locked in positions pointing away from the alkynyl substituents avoiding steric interactions. This also allows for full planarity of the methoxy substituents with the aromatic core. This is the optimum position for overlap of the *p*-orbital lone pair of the oxygen atoms with the  $\pi$ -orbitals of the benzene ring.<sup>[26]</sup>

In **7** the two trimethylsilyl groups have their methyl groups placed in an “extended” staggered conformation with respect to each other. That is, the methyl groups are placed as far away from each other as possible in the crystal structure.

The methoxy substituents are highly electron-donating but also space filling and these two effects could render the ethynyl bromides relatively stable.

## Optical Spectroscopy

The UV/Vis spectra of 1,4-benzoquinone, 2,3-diiodo-1,4-benzoquinone (**11**) and the three 2,3-dialkynyl-1,4-benzoquinones **8**, **9** and **10** recorded in acetonitrile are depicted in Figure 4. The spectrum of 1,4-benzoquinone shows a band at 241 nm and a close inspection of the spectrum reveals a weak band at approximately 280 nm. Three bands are found in the spectrum of 2,3-diiodo-1,4-benzoquinone (**11**), but these are red-shifted in comparison to the spectrum of 1,4-benzoquinone and occurs at approximately 265, 319 and 405 nm and the low-energy band has a significantly stronger intensity relative to the high-energy bands in comparison to the spectrum of 1,4-benzoquinone. This low-energy band is found at approximately the same wavelength in the spectrum of the TMS-alkyne-substituted quinone **10** but here the band at approximately 320 nm is absent. The UV/Vis spectra of the two alkynyl-substituted quinones **8** and **9** are almost identical to the spectrum of the TMS-alkyne-substituted analog **10**. The main difference between **8** and **9** as compared to **10** is the position of the low-energy band (at ca. 400 nm), which is blue-shifted by approximately 10 nm in **10**.

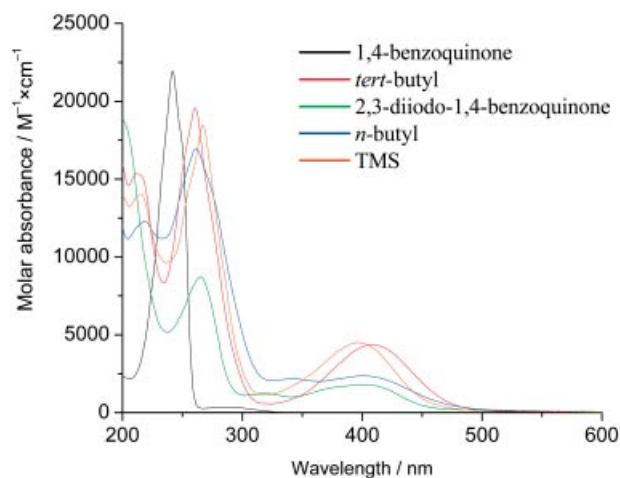


Figure 4. UV/Vis spectra of all 1,4-benzoquinones in this study.

## Electrochemistry

The reduction of the three 2,3-dialkynyl-1,4-benzoquinones **8–10** and of two reference compounds, 1,4-benzoquinone and 2,3-dioctyl-1,4-benzoquinone,<sup>[22]</sup> was investigated by slow-sweep cyclic voltammetry in MeCN with  $Bu_4NPF_6$  (0.1 M) as the supporting electrolyte. The voltammogram obtained for **8**, typical for the whole series, is shown in Figure 5 and the data for all five compounds are summarized in Table 2. The first one-electron reduction resulting in the formation of the radical anion appeared in all cases as a quasi-reversible redox couple (R1/O1), whereas the further reduction to the dianion was essentially irreversible (R2/O2). These observations are in good agreement with results obtained earlier for 1,4-benzoquinone and a number of substituted derivatives.<sup>[27–30]</sup>

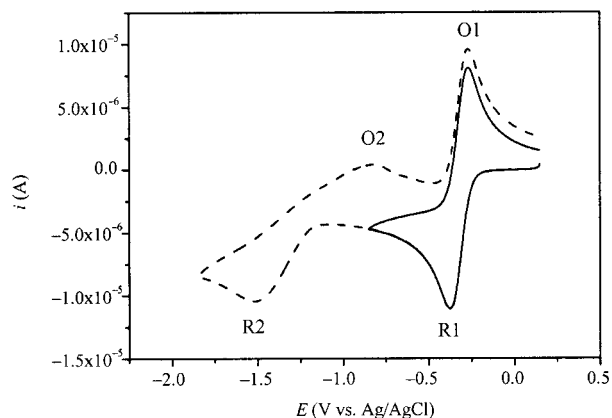


Figure 5. Cyclic voltammograms for the reduction of **8** (2 mM) in MeCN/ $\text{Bu}_4\text{NPF}_6$  (0.1 M) at  $\nu = 0.1 \text{ V s}^{-1}$  and with the direction of the voltage scan being reversed at  $-0.85 \text{ V}$  (solid line) and  $-1.85 \text{ V}$  (dashes), respectively.

Table 2. Cyclic voltammetry data for the reduction of the 2,3-dialkynyl-1,4-benzoquinones **8–10** and two selected reference compounds.

Substrate	$E^{\circ'}$ [a]	$E_{\text{p}}^{\text{red}}$ [b]	$i_{\text{p}}^{\text{red}}$ [c]	$D_{\text{o}}^{\text{red}}$ [d]
1,4-Benzoquinone	-0.47	-1.75	$9.3 \cdot 10^{-6}$	1
2,3-Dioctyl-1,4-benzoquinone	-0.59	-1.78	$4.6 \cdot 10^{-6}$	0.24
2,3-Di(hex-1-ynyl)-1,4-benzoquinone ( <b>8</b> )	-0.32	-1.52	$9.5 \cdot 10^{-6}$	1.04
2,3-Bis(3,3-dimethylbut-1-ynyl)-1,4-benzoquinone ( <b>9</b> )	-0.34	-1.58	$9.5 \cdot 10^{-6}$	1.04
2,3-Bis(trimethylsilylethynyl)-1,4-benzoquinone ( <b>10</b> )	-0.22	-1.36	$8.5 \cdot 10^{-6}$	0.84

[a] Potentials are in given in V vs. Ag/AgCl (3 M NaCl) and currents in A. Formal potential for the first reduction wave (R1) determined as the average of the peak potentials for reduction and oxidation, ( $E_{\text{p}}^{\text{red}} = +E_{\text{p}}^{\text{ox}}/2$ ). [b] Peak potential for the second reduction wave (R2). [c] Peak current for the first reduction wave (R1). [d] Diffusion coefficient relative to that for 1,4-benzoquinone determined from the values of  $i_{\text{p}}^{\text{red}}$  and Equation (1).

From the formal potentials for the first redox couple it is seen that 2,3-dioctyl-1,4-benzoquinone is more difficult to reduce than the parent 1,4-benzoquinone ( $\Delta E^{\circ'} = -0.12 \text{ V}$ ), whereas the three 2,3-dialkynyl-1,4-benzoquinones **8–10**, are all more easily reduced ( $\Delta E^{\circ'} = 0.15 \text{ V}$ ,  $0.13 \text{ V}$  and  $0.25 \text{ V}$ , respectively). This trend is paralleled by the data for the second redox couple. However, it is well known that the thermodynamics and the kinetics associated with the second electron transfer for 1,4-benzoquinones are strongly dependent on both the nature of the supporting electrolyte cation<sup>[29]</sup> and the ability of the solvent to act as a hydrogen-bond donor.<sup>[30]</sup> Thus, the potentials recorded for the second redox couple result from a complex interplay between internal and external effects and we shall, for that reason, restrict the short discussion to follow to include only the data for the first electron transfer.

The effect of substitution on the reduction potential for 1,4-benzoquinones has been addressed in a number of cases.<sup>[31–34]</sup> The Hammett  $\rho$ -values are positive and typically close to 6.5. In other words, and as intuitively expected, the introduction of electron-donating substituents makes re-

duction of the quinone more difficult, whereas the introduction of electron-withdrawing substituents makes reduction easier. This trend is in agreement with the data in Table 2.

In more quantitative terms, the electrochemical reduction involves the transfer of an electron to the lowest unoccupied molecular orbital (LUMO) and the possible correlation between reduction potentials and LUMO energies,  $E_{\text{LUMO}}$ , has been addressed for more than 40 years.<sup>[35]</sup> Typically, linear correlations are observed when the substrates all belong to the same class of compounds, e.g., substituted 1,4-quinones,<sup>[32–38]</sup> where the structural changes and the solvent reorganization that accompany the electron transfer vary gradually with changes in, for instance,  $E_{\text{LUMO}}$ . Similarly, linear relationships between the formal potentials for reduction and UV/Vis spectroscopic  $1/\lambda_{\text{max}}$  values are frequently observed.<sup>[39–41]</sup> Although the present work is only a part of a larger investigation focused on the chemistry of 2,3-dialkynyl-1,4-benzoquinones we prefer already at this stage to test for such correlations between the formal reduction potentials and other related electronic data.

Initially, we investigated the correlations between  $E^{\circ'}$  for the first electron transfer vs.  $E_{\text{LUMO}}$  and  $1/\lambda_{\text{max}}$ . However, we did not observe a general linear relationship between  $E^{\circ'}$  and  $E_{\text{LUMO}}$  or  $E^{\circ'}$  and  $1/\lambda_{\text{max}}$  for the reduction of the quinones but by leaving out 1,4-benzoquinone thus considering only the four 2,3-disubstituted derivatives, we observed a linear relationship between  $E^{\circ'}$  and  $1/\lambda_{\text{max}}$  and also between  $E^{\circ'}$  and  $E_{\text{LUMO}}$ . This finding indicates that solvation affects the stability of the radical anions and the excited states in a similar fashion.

In order to elaborate on the solvation effect we have also investigated the relation between  $E^{\circ'}$  and the calculated electron affinities (EAs) for the benzoquinones (see below for details of the calculations). In the hypothetical case where the effect of solvation is constant throughout the series we would expect a linear correlation between values of EA and  $E^{\circ}$ .<sup>[42,43]</sup> Indeed, a reasonable linear correlation is observed (Figure 6), however, with a slope of 0.59 sug-

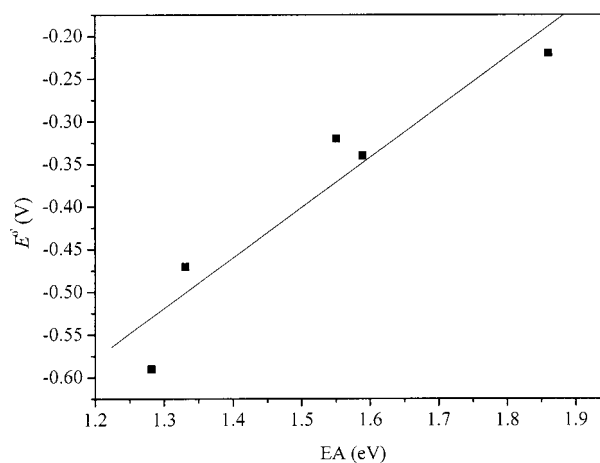


Figure 6. Plot of the  $E^{\circ'}$  for one-electron reduction of the 1,4-benzoquinones (Table 2) as a function of the calculated electron affinities (EAs).

gesting a noticeable substituent effect on the solvation of the benzoquinones.

The height of a voltammetric reduction peak,  $i_p^{\text{red}}$ , is given by Equation (1),<sup>[44]</sup> where  $A$  is the electrode area,  $C_o^*$  and  $D_o$  are the bulk concentration and the diffusion coefficient of the substrate, respectively,  $v$  is the voltage sweep rate,  $n$  is the number of electrons transferred, here  $n = 1$ , and  $T$  is the absolute temperature. Thus, since all the parameters except  $D_o$  are known, a measured value of  $i_p^{\text{red}}$  would in principle give access to the value of  $D_o$ . However, although the geometric area of the working electrode is, of course, known the microscopic area to be used in Equation (1) is rarely known to the accuracy needed for good estimates of  $D_o$ . Instead the data treatment usually includes the determination of the relative values; here we have chosen the unsubstituted 1,4-benzoquinone as the standard compound.

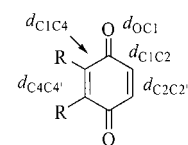
$$i_p^{\text{red}} = 0.4463nFA C_o^* D_o^{1/2} v^{1/2} (nF/RT)^{1/2} \quad (1)$$

Values of the relative diffusion coefficients,  $D_o^{\text{rel}}$ , are given in Table 2 and it can be seen that the diffusion coefficients for the series of quinones investigated in this study are indeed, with the exception of that for 2,3-dioctyl-1,4-benzoquinone, very similar. This may at first glance seem surprising considering the large structural change in passing from the unsubstituted 1,4-benzoquinone to **8**, **9** and **10**, respectively. We see this as the result of two opposing effects. On the one hand, it would be expected that the larger the substrate, the smaller the diffusion coefficient, but on the other, it would be expected also that the solvation shell is less tight for the 2,3-dialkynyl-1,4-benzoquinones and this would predict a larger diffusion coefficient. This again points to the importance of solvation effects in determining the energies of the quinone redox systems, even in aprotic solvents. In contrast, the value of  $D_o^{\text{rel}}$  for 2,3-dioctyl-1,4-benzoquinone is considerably smaller than those for the other compounds in the series. Most likely this reflects the flexibility of the two octyl groups.

## Calculations

Geometry optimizations were carried out at the B3LYP/6-31G(d) level of theory, where  $C_{2v}$  symmetry was imposed on all the molecules. The obtained molecular structures were confirmed to be minima on the potential energy surface by carrying out a subsequent calculation of the frequencies for each molecule. Selected bond lengths are shown in Figure 7.

The conjugation “pathway” O–C1–C2–C2–C1–O (see Figure 7) is 6.75–6.77 Å in all cases with only slight variation in the bond lengths, whereas the pathway O–C1–C4–C4–C1–O is slightly longer (6.77–6.83 Å). This slight distortion of the benzoquinone skeleton reflects the changes in the geometry of the substituents on the benzoquinone ring and since this distortion is small, the observed differences in the electronic properties should be due to the different electron-donating and -accepting properties of the



	$d_{OC1}$	$d_{C1C2}$	$d_{C2C2'}$	$d_{C1C4}$	$d_{C4C4'}$
1,4-Benzoquinone	1.225	1.487	1.343	1.487	1.343
2,3-Dioctyl-1,4-benzoquinone	1.227	1.482	1.336	1.499	1.369
2,3-Di(hex-1-ynyl)-1,4-benzoquinone ( <b>8</b> )	1.224	1.484	1.340	1.501	1.377
2,3-Bis(3,3-dimethyl-but-1-ynyl)-1,4-benzoquinone ( <b>9</b> )	1.224	1.484	1.340	1.501	1.378
2,3-Bis(trimethylsilyl-ethynyl)-1,4-benzoquinone ( <b>10</b> )	1.223	1.483	1.340	1.503	1.377

Figure 7. Selected bond lengths [Å] in the benzoquinone skeleton.

substituents and not reflect differences in the benzoquinone  $\pi$ -conjugated system.

TD-DFT calculations were then carried out (again at the B3LYP/6-31G(d) level of theory). In all the calculations the molecules were placed in the xy plane. The vertical excitation energies and dipole moments obtained from these calculations are summarized in Table 3. A slight shift in the excitation energies are observed as a function of the substitution patterns on the quinones: The Si containing analog **10** has slightly higher excitation energy in comparison to the two alkyl analogs **8** and **9** in agreement with the UV/Vis data, where we observed a blue shift of 10 nm of the band occurring at approximately 400 nm for **10**. Differences in the calculated dipole moments bears these findings out: The dipole moment is higher in the alkyl analogs **8** and **9** as compared to the TMS-analog **10**. This difference is simply interpreted to be due to the difference in electronegativity of C and Si.

Table 3. Calculated excitation energies and dipole moments.

Molecule	Excitation energy [eV]	Electron affinity [eV]	LUMO [eV]	Dipole moment [Debye]
<b>8</b>	2.42	1.55	−3.29	2.63
<b>9</b>	2.41	1.59	−3.30	2.58
<b>10</b>	2.48	1.86	−3.52	1.90
1,4-Benzoquinone	2.47	1.33	−3.54	0.00
2,3-Dioctyl-1,4-benzoquinone	2.40	1.28	−3.21	0.87

Furthermore, we calculated the adiabatic electron affinities (EA) of the studied benzoquinones: Single-point calculations on the anion radicals were carried out, where the geometries from the neutral structures were used. The difference in the electronic energy between the anion radical and the neutral structure is defined as the adiabatic electron affinity. The correlation between the EAs and the reduction potentials is discussed above.

In the results presented above we have argued that the alkynyl substituent serves as an electron-withdrawing group. To further support this finding we have investigated the electron densities of the HOMO and LUMO orbitals of 1,4-benzoquinone, 2,3-dioctyl-1,4-benzoquinone and **10**. The densities are presented in Figure 8.

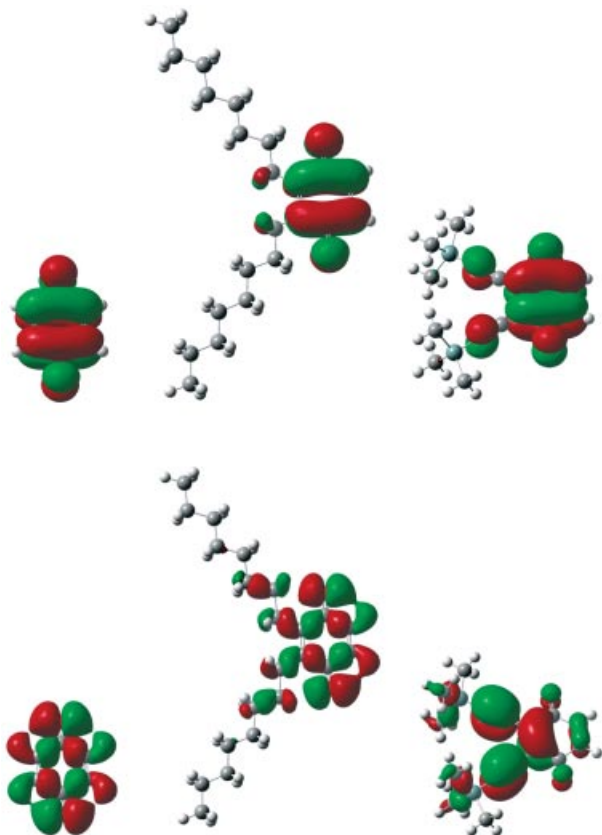


Figure 8. Electron-density plots of the LUMOs (top) and HOMOs (bottom) of 1,4-benzoquinone, 2,3-dioctyl-1,4-benzoquinone and **10**, respectively (from left to right).

In the plots of the HOMOs of 1,4-benzoquinone and 2,3-dioctyl-1,4-benzoquinone we see that the electron density is evenly spread out across the benzoquinone system – only small variations are observed in the density for 2,3-dioctyl-1,4-benzoquinone as compared to 1,4-benzoquinone. The HOMO for **10** is significantly different from the two others and we observe that the electron density is mainly located at the triple bonds and at the carbon atoms on the benzoquinone ring adjacent to the triple bonds. A noticeably amount of the electron density is also found at the tertiary carbon atoms in the *tert*-butyl group. The LUMOs of all three compounds more or less look the same characterized by a single nodal plane. Some density is present on the triple bonds in the LUMO of **10**. Most electronic transitions in organic molecules are characterized as LUMO–HOMO transitions and from the density studies above we observe that for 2,3-dioctyl-1,4-benzoquinone this transition is mainly localized at the 1,4-benzoquinone system, whereas for **10** charge is transferred from the more electron-rich triple bonds into the 1,4-benzoquinone system. From these

observations we deduce that the alkyne functionality is in fact electron-withdrawing as it is the electron-rich part of the 1,4-benzoquinone in the HOMO–LUMO transition.

## Conclusions

A convenient method for the synthesis of 2,3-dialkynyl-1,4-benzoquinones is described. The electrochemical and optical results show clearly that alkynyl substituents are electron-withdrawing. This observation was confirmed by DFT calculations. This is apparently, this aspect has been overlooked by many of the groups working with molecular wires based on hole-transport, where the transport-properties are likely to be affected by the presence of acceptor groups in the conduction path of the wire. Future synthetic efforts will be directed towards the incorporating of such synthetic building blocks into larger aromatic systems for applications in nonlinear optics and liquid crystals.

## Experimental Section

**General Methods:** Unless otherwise stated, all starting materials were obtained from commercial suppliers and used as received. Solvents were HPLC grade and were used as received.  $^1\text{H}$  NMR and  $^{13}\text{C}$  NMR spectra were recorded on a 300 MHz NMR (Varian) apparatus (300 MHz for  $^1\text{H}$  NMR and 75 MHz for  $^{13}\text{C}$  NMR) or on a 400 MHz NMR (Bruker) apparatus (400 MHz for  $^1\text{H}$  NMR and 100 MHz for  $^{13}\text{C}$  NMR). Proton chemical shifts are reported in ppm downfield from tetramethylsilane (TMS) and carbon chemical shifts in ppm downfield of TMS using the resonance of the deuterated solvent as internal standard ( $\delta = 76.9$  ppm for  $\text{CDCl}_3$ ). Elemental analysis was performed by Mrs Birgitta Kegel at the Microanalytical Laboratory at the Department of Chemistry, University of Copenhagen. Fast-atom bombardment (FAB) mass spectra were recorded on a Jeol JMS-HX 110A Tandem Mass Spectrometer in the positive ion mode using *m*-NBA (*m*-nitrobenzyl alcohol) as the matrix. Gas chromatography-mass spectrometry (GC-MS) was performed with a HP5890 Series II plus gas chromatograph coupled with a HP5872 Series Mass analyser. Dry column vacuum chromatography<sup>[45]</sup> was performed using 15–40 mesh silica from Merck. UV-vis spectra were recorded using a Perkin-Elmer Lambda2 spectrometer. A Personal Chemistry, Smith Creator oven was employed for microwave-assisted reactions.

CCDC-292850 and -292851 contain the supplementary crystallographic data for this paper. These data can be obtained free of charge from The Cambridge Crystallographic Data Centre via [www.ccdc.cam.ac.uk/data\\_request/cif](http://www.ccdc.cam.ac.uk/data_request/cif).

**Calculations:** The Gaussian 03 suite of programs<sup>[46]</sup> was used for the DFT calculations. Initially, geometry optimizations were carried out at the B3LYP/6-31G(d) level of theory, where all the structures were constrained to  $C_{2v}$  symmetry. Frequency calculations were then carried out to assure that the structures were indeed minima on the potential energy surface (no imaginary frequencies). TD-DFT calculations and single point calculations on the anion radicals were then carried out at the B3LYP/6-31G(d) level of theory on these optimized structures. The Gaussian archive entries for these calculations are included in the supplementary information. GaussView 3.0<sup>[47]</sup> was used for generating the orbital plots.

**Cyclic Voltammetry:** Tetrabutylammonium hexafluorophosphate,  $\text{Bu}_4\text{NPF}_6$  (Aldrich, 98%) and acetonitrile, MeCN (Lab-Scan,

HPLC grade) were used as received. The cell and electrodes for cyclic voltammetry were from BAS. The cell was a cylindrical vial (MF-1052) equipped with a Teflon top with holes to accommodate the Pt working electrode (MF-2013,  $d = 1.6$  mm), the Pt counter electrode (MW-4130) and the Ag/AgCl (3 M NaCl) reference electrode (RE-5B). The electrochemical equipment was from ECO (Autolab), including the PSTAT10 potentiostat (without  $iR$ -compensation). The solutions for voltammetry were 2 mM in substrate and made by dissolving an accurately weighed amount of the substrate in the required volume of a MeCN/Bu<sub>4</sub>NPF<sub>6</sub> (0.1 M) solution. The volume of the resulting solutions was typically between 5 and 10 mL. The solutions were purged with nitrogen saturated with MeCN for at least 10 min prior to the measurements. The peak potentials ( $E_p$ ) were determined by the ECO Autolab software (GPES, vers. 4.9).

**1,4-Dimethoxy-2,3-dinitrobenzene (2):** 1,4-Dimethoxybenzene (100 g, 0.72 mmol) was dissolved in ice cooled 62% HNO<sub>3</sub> (1000 mL) during 30 minutes. The mixture was stirred for 1 hour at 0 °C, at room temperature for 1 hour and at 100 °C for 1 hour. The reaction mixture was poured into ice water (2 L) and the yellow solid material was filtered off, washed with water and air-dried. The yellow precipitate was recrystallized twice from 1.5 L glacial acetic acid to yield the pure 2,3-dinitro isomer. Yield: 148.6 g, 90%. M.p. 184–186 °C. <sup>1</sup>H NMR (CDCl<sub>3</sub>):  $\delta = 3.94$  (s, 6 H), 7.20 (s, 2 H) ppm. <sup>13</sup>C NMR (CDCl<sub>3</sub>):  $\delta = 57.4, 116.6, 134.3, 145.2$  ppm. MS (GC-MS):  $m/z = 228$ .

**1,2-Diamino-3,6-dimethoxybenzene (3):** Dinitro compound **2** (5.0 g, 21.9 mmol) was dissolved in EtOAc (96%, 100 mL) and added to Pd/C (100 mg, 10%). This mixture was hydrogenated at 5 bar for 24 hours. The reaction mixture was filtered through a plug of celite and evaporate to dryness in vacuo. This yielded a dark grey solid material that was pure by GC-MS analysis. The crude was purified by dry column vacuum chromatography (heptane to EtOAc with 10% increments) to yield an off-white solid. Yield: 3.67 g, 99%. M.p. 86–87 °C. <sup>1</sup>H NMR (CDCl<sub>3</sub>):  $\delta = 3.21$  (br. s, 4 H), 3.75 (s, 6 H), 6.22 (br. s, 2 H) ppm. MS (GC-MS):  $m/z = 168$ .

**2,3-Diiodo-1,4-dimethoxybenzene (4):** A solution of diamino compound **3** (27 g, 0.16 mol) in ice cold concentrated H<sub>2</sub>SO<sub>4</sub> (500 mL) was added over 30 minutes at 0 °C to a stirred solution of nitrosyl sulfuric acid (prepared from 44.4 g (0.64 mol) NaNO<sub>2</sub> and 500 mL concentrated H<sub>2</sub>SO<sub>4</sub> according to Fierz-David and Blangey<sup>[17]</sup>) resulting in a red solution. Stirring was continued at 0 °C for an additional 20 minutes. Phosphoric acid (85%, 625 mL) was added slowly to the solution and the temperature was kept below 10 °C (20 minutes in ice bath) and then stirred for an additional 20 minutes. The resulting yellow inhomogeneous slurry was poured into a violently stirred solution of KI (120 g, 0.72 mol) in ice water (3000 mL). This gave a deep red solution and some gas evolution. This solution was stirred at room temperature for 2 hours and then heated to 40 °C for 30 minutes. The solution was extracted with CH<sub>2</sub>Cl<sub>2</sub> (3 × 1000 mL) and the combined organic phases were washed with aqueous bisulfite, dried (MgSO<sub>4</sub>), filtered and evaporate to dryness in vacuo. The resulting residue was taken up in CH<sub>2</sub>Cl<sub>2</sub> and filtered through a short plug of silica. This yields the (almost) pure diiodide as seen by GC-MS. Dry column vacuum chromatography (heptane to 1:1 heptane/EtOAc with 5% increments) yields the pure target molecule as a white solid material. Yield: 60%, 37.5 g. M.p. 166–168 °C. <sup>1</sup>H NMR (CDCl<sub>3</sub>):  $\delta = 3.84$  (s, 6 H), 6.87 (s, 2 H) ppm. <sup>13</sup>C NMR (CDCl<sub>3</sub>):  $\delta = 57.3, 102.6, 110.9, 154.0$  ppm. MS (GC-MS):  $m/z = 390$ . C<sub>8</sub>H<sub>8</sub>I<sub>2</sub>O<sub>2</sub> (389.96): C 24.64, H 2.07; found: C 24.84, H 2.21.

**2,3-Bis(hex-1-ynyl)-1,4-dimethoxybenzene (5):** Diiodide **4** (395 mg, 1.0 mmol) and Pd(PPh<sub>3</sub>)<sub>4</sub> (115 mg, 0.10 mmol) was suspended in a

mixture of degassed anhydrous DMF (4.5 mL) and degassed Et<sub>2</sub>NH (4.5 mL). To this suspension CuI (75 mg) was added. The MW vial was closed and 1-hexyne (185 mg) was added via syringe and the mixture was heated in the MW (settings: 120 °C, 15 bar, 200 W, powermax off) for 10 minutes. The reaction mixture was poured into 2 M HCl (25 mL), extracted with CH<sub>2</sub>Cl<sub>2</sub> (3 × 25 mL), dried (MgSO<sub>4</sub>), filtered and the solvents evaporated to dryness in vacuo. The residue was purified by dry column vacuum chromatography (heptane to toluene with 5% increments) to give a pale yellow solid. Yield: 257 mg, 85%. M.p. 31–32 °C. <sup>1</sup>H NMR (CDCl<sub>3</sub>):  $\delta = 0.97$  (t, 6 H), 1.50–1.59 (m, 4 H), 1.60–1.69 (m, 4 H), 2.65 (t, 4 H), 3.82 (s, 6 H), 6.71 (s, 2 H). <sup>13</sup>C NMR (CDCl<sub>3</sub>):  $\delta = 13.6, 19.7, 21.9, 30.9, 56.4, 75.4, 98.8, 110.5, 117.3, 154.2$  ppm. MS (GC-MS):  $m/z = 298$ . C<sub>20</sub>H<sub>26</sub>O<sub>2</sub> (298.43): C 80.50, H 8.78; found: C 80.34, H 8.98.

**2,3-Bis(3,3-dimethylbut-1-ynyl)-1,4-dimethoxybenzene (6):** Diiodide **4** (300 mg, 0.77 mmol) and Pd(PPh<sub>3</sub>)<sub>4</sub> (65 mg, 0.056 mmol) was suspended in a mixture of degassed anhydrous DMF (4.5 mL) and degassed Et<sub>2</sub>NH (4.5 mL). To this suspension CuI (50 mg) was added. The MW vial was closed and the alkyne (2.31 mmol, 190 mg) was added via syringe and the mixture was heated in the MW (settings: 120 °C, 15 bar, 200 W, powermax off) for 10 minutes. The reaction mixture was poured into 2 M HCl (20 mL), extracted with CH<sub>2</sub>Cl<sub>2</sub> (3 × 25 mL), dried (MgSO<sub>4</sub>), filtered and the solvents evaporated to dryness in vacuo. The residue was purified by dry column vacuum chromatography (heptane to EtOAc with 2% increments) to give a pale yellow solid. Yield: 185 mg, 80%. M.p. 78–79 °C. <sup>1</sup>H NMR (CDCl<sub>3</sub>):  $\delta = 1.34$  (s, 18 H), 3.80 (s, 6 H), 6.70 (s, 2 H). <sup>13</sup>C NMR (CDCl<sub>3</sub>):  $\delta = 28.3, 31.2, 56.8, 74.2, 107.0, 111.8, 117.8, 154.7$  ppm. MS (GC-MS):  $m/z = 298$ . C<sub>20</sub>H<sub>26</sub>O<sub>2</sub> (298.43): C 80.50, H 8.78; found: C 79.98, H 9.00.

**(3,6-Dimethoxy-1,2-phenylene)bis(ethyne-2,1-diyl)bis(trimethylsilane) (7):** Diiodide **4** (3.0 g, 7.7 mmol) and Pd(PPh<sub>3</sub>)<sub>4</sub> (900 mg, 0.7 mmol, 20 mol-%) was suspended in a mixture of degassed anhydrous DMF (20 mL) and degassed Et<sub>2</sub>NH (20 mL). To this suspension CuI (700 mg) was added. The MW vial was closed and the alkyne (2.27 mL, 23.1 mmol) was added via syringe and the mixture was heated in the MW (settings: 120 °C, 15 bar, 200 W, powermax off) for 20 minutes. The reaction mixture was poured into 2 M HCl (200 mL) and the mixture was extracted with CH<sub>2</sub>Cl<sub>2</sub> (3 × 150 mL), dried (MgSO<sub>4</sub>), filtered and the solvents evaporated to dryness in vacuo. The crude compound was purified by two consecutive columns (on silica) using the dry column vacuum chromatography technique (1% gradient from heptane to EtOAc; then heptane to toluene with 10% increments) to give a crystalline material. This was recrystallized from cold heptane to yield a colorless crystalline material. Yield: 1.65 g, 65%. M.p. 76–77 °C. <sup>1</sup>H NMR (CDCl<sub>3</sub>):  $\delta = 0.28$  (s, 18 H), 3.81 (s, 6 H), 6.76 (s, 2 H) ppm. <sup>13</sup>C NMR (CDCl<sub>3</sub>):  $\delta = 0.05, 56.5, 99.1, 103.3, 112.0, 116.6, 154.7$  ppm. MS (GC-MS):  $m/z = 330$ . C<sub>18</sub>H<sub>26</sub>O<sub>2</sub>Si<sub>2</sub> (330.57): C 65.40, H 7.93; found: C 65.80, H 8.06.

**2,3-Bis(hex-1-ynyl)cyclohexa-2,5-diene-1,4-dione (8):** Dimethoxy compound **5** (300 mg, 1.01 mmol) was dissolved in acetonitrile (20 mL) and CAN (1.65 g, 3.03 mmol, 3 equiv.) dissolved in water (20 mL) was added during 5 minutes at room temperature. The homogeneous solution was stirred for 20 minutes and additional water was added (40 mL). The mixture was extracted with CH<sub>2</sub>Cl<sub>2</sub> (3 × 40 mL), dried (MgSO<sub>4</sub>) and filtered through paper. The resulting yellow solution was filtered through a plug of silica and the solvents evaporated to dryness in vacuo to yield the target compound as a yellow solid. Yield: 254 mg, 94%. M.p. 26–28 °C. <sup>1</sup>H NMR (CDCl<sub>3</sub>):  $\delta = 0.95$  (t, 6 H), 1.42–1.59 (m, 4 H), 1.61–1.69

(m, 4 H), 2.58 (t, 4 H), 6.75 (s, 2 H) ppm.  $^{13}\text{C}$  NMR ( $\text{CDCl}_3$ ):  $\delta$  = 14.5, 20.1, 21.8, 30.2, 75.3, 111.4, 132.5, 136.5, 183.0 ppm. MS (GC-MS):  $m/z$  = 268.  $\text{C}_{18}\text{H}_{20}\text{O}_2$  (268.36): C 80.56, H 7.51; found: C 80.76, H 7.73.

**2,3-Bis(3,3-dimethylbut-1-ynyl)cyclohexa-2,5-diene-1,4-dione (9):** Dimethoxy compound **6** (80 mg, 0.27 mmol) was dissolved in acetonitrile (5 mL) and CAN (441 mg, 0.80 mmol, 3 equiv.) dissolved in water (5 mL) was added during 5 minutes at room temperature. The homogeneous solution was stirred for 5 minutes and additional water was added (25 mL). The mixture was extracted with  $\text{CH}_2\text{Cl}_2$  ( $3 \times 15$  mL), dried ( $\text{MgSO}_4$ ) and filtered through paper. The resulting yellow solution was filtered through a plug of silica and the solvents evaporated to dryness in vacuo to yield the target compound as a yellow solid. Yield: 68 mg, 95%. M.p. 63–64 °C.  $^1\text{H}$  NMR ( $\text{CDCl}_3$ ):  $\delta$  = 1.37 (s, 18 H), 6.72 (s, 2 H) ppm.  $^{13}\text{C}$  NMR ( $\text{CDCl}_3$ ):  $\delta$  = 28.9, 30.5, 73.9, 118.7, 132.2, 136.4, 182.8 ppm. MS (GC-MS):  $m/z$  = 268.  $\text{C}_{18}\text{H}_{20}\text{O}_2$  (268.36): C 80.56, H 7.51; found: C 79.97, H 7.59.

**2,3-Bis(trimethylsilyl)ethynylcyclohexa-2,5-diene-1,4-dione (10):** Dimethoxy compound **7** (0.34 g, 1.0 mmol) was dissolved in acetonitrile (60 mL) and CAN (1.8 g, 3.3 eqv, 3.3 mmol) was added dissolved in water (60 mL). The reaction mixture was stirred for 20 minutes at room temperature to give an orange solution. Additional water (60 mL) was added and the reaction mixture was extracted with  $\text{CH}_2\text{Cl}_2$  ( $3 \times 50$  mL), dried ( $\text{MgSO}_4$ ), filtered through paper and the solvents evaporated to dryness. The crude orange oil was purified by dry column vacuum chromatography (heptane to 20% EtOAc in heptane with 2% increments) to leave the target compound as a low melting yellow solid material. Yield: 0.28 g, 92%. M.p. 76–77 °C.  $^1\text{H}$  NMR ( $\text{CDCl}_3$ ):  $\delta$  = 0.29 (s, 18 H), 6.76 (s, 2 H) ppm.  $^{13}\text{C}$  NMR ( $\text{CDCl}_3$ ):  $\delta$  = -0.46, 97.3, 117.2, 132.3, 136.5, 182.3 ppm. MS (GC-MS):  $m/z$  = 300.  $\text{C}_{16}\text{H}_{20}\text{O}_2\text{Si}_2$  (300.50): C 63.45, H 6.71; found: C 63.51, H 6.73.

**2,3-Diiodo-1,4-benzoquinone (11):** Diiodo dimethoxy compound **4** (200 mg, 0.51 mmol) was dissolved in acetonitrile (5 mL), then CAN (840 mg, 3 equiv., 1.54 mmol) dissolved in water (5 mL), was added. The reaction mixture was stirred for 20 minutes at room temperature leaving an orange solution. Additional water (20 mL) was added and the reaction mixture was extracted with  $\text{CH}_2\text{Cl}_2$  ( $3 \times 30$  mL), dried ( $\text{MgSO}_4$ ), filtered through paper and the solvents evaporated to dryness. The crude orange oil was purified by dry column vacuum chromatography (heptane to 20% EtOAc in heptane with 2% increments) to leave the target compound as a red solid material. Yield: 179 mg, 97%. M.p. 154–155 °C.  $^1\text{H}$  NMR ( $\text{CDCl}_3$ ):  $\delta$  = 7.11 (s, 2 H) ppm.  $^{13}\text{C}$  NMR ( $\text{CDCl}_3$ ):  $\delta$  = 133.8, 135.3, 177.6 ppm. MS (GC-MS):  $m/z$  = 360.  $\text{C}_6\text{H}_2\text{I}_2\text{O}_2$  (359.89): C 20.02, H 0.56; found: C 20.30, H 0.62.

**2,3-Bis(bromoethynyl)-1,4-dimethoxybenzene (12):** Di-TMS compound (**7**) (200 mg, 6.05 mmol) was dissolved in anhydrous acetone (10 mL) and NBS (215 mg, 12.1 mmol) was added followed by  $\text{AgNO}_3$  (41 mg, 0.2 mmol). The reaction mixture was stirred at room temperature for 4 hours. The volatiles were removed in vacuo and the residue was purified by dry column vacuum chromatography (heptane to EtOAc with 5% increments) to yield the target compound as a white solid material. Yield 151 mg, 73%. M.p. 131–132 °C (decomposes).  $^1\text{H}$  NMR ( $\text{CDCl}_3$ ):  $\delta$  = 3.82 (s, 6 H), 6.79 (s, 2 H) ppm.  $^{13}\text{C}$  NMR ( $\text{CDCl}_3$ ):  $\delta$  = 55.4, 57.8, 74.6, 111.7, 116.4, 154.8 ppm. MS (GC-MS):  $m/z$  = 344.  $\text{C}_{12}\text{H}_8\text{Br}_2\text{O}_2$  (344.00): C 41.90, H 2.34; found: C 42.25, H 2.17.

**Supporting Information** (see also the footnote on the first page of this article): Input files used for the TD-DFT calculations on com-

pounds **8**, **9**, **10**, 1,4-benzoquinone and 2,3-dioctyl-1,4-benzoquinone.

## Acknowledgments

This work would not have been possible without the discussions with students and staff members at the Department of Chemistry, University of Copenhagen.

- [1] E. Conwell (Ed.), *Semiconductors and Semimetals: Highly Conducting Quasi-One-Dimensional Organic Crystals*, Academic Press, Boston, **1988**, vol. 27.
- [2] T. Murata, Y. Morita, K. Fukui, K. Sato, D. Shiomi, T. Takui, M. Maesato, H. Yamochi, G. Saito, K. Nakasuji, *Angew. Chem. Int. Ed.* **2004**, *43*, 6343.
- [3] R. Bentley, I. M. Campbell, in: *The Chemistry of the Quinoid Compounds, Part 2* (Ed.: S. Patai), John Wiley & Sons, London, **1974**, chapter 13.
- [4] H. Sies, L. Packer (Eds.), *Methods in Enzymology*, Elsevier, Amsterdam, **2004**, vol. 378.
- [5] H. Sies, L. Packer (Eds.), *Methods in Enzymology*, Elsevier, Amsterdam, **2004**, vol. 382.
- [6] T. Nishinaga, Y. Miyata, N. Nodera, K. Komatsu, *Tetrahedron* **2004**, *60*, 3375.
- [7] K. C. Nicolaou, A. Liu, Z. Zeng, S. McComb, *J. Am. Chem. Soc.* **1992**, *114*, 9279.
- [8] H. W. Moore, K. F. West, U. Wriede, K. Chow, M. Fernandez, N. V. Nguyen, *J. Org. Chem.* **1987**, *52*, 2537.
- [9] N. Choy, K. C. Russel, J. C. Alvarez, A. Fider, *Tetrahedron Lett.* **2000**, *41*, 1515–1518.
- [10] C. Hansch, A. Leo, R. W. Taft, *Chem. Rev.* **1991**, *91*, 165–195.
- [11] R. E. Martin, J. A. Wytko, F. Diederich, C. Boudon, J.-P. Gisselbrecht, M. Gross, *Helv. Chim. Acta* **1999**, *82*, 1470.
- [12] N. N. P. Moonen, C. Boudon, J.-P. Gisselbrecht, P. Seiler, M. Gross, F. Diederich, *Angew. Chem. Int. Ed.* **2002**, *41*, 3044.
- [13] A. Auffrant, F. Diederich, C. Boudon, J.-P. Gisselbrecht, M. Gross, *Helv. Chim. Acta* **2004**, *87*, 3085.
- [14] G. H. Fisher, H. R. Moreno, J. E. Oatis Jr, H. P. Schultz, *J. Med. Chem.* **1975**, *18*, 746.
- [15] C. Flader, J. Liu, R. F. Borch, *J. Med. Chem.* **2000**, *43*, 3157.
- [16] J. N. H. Reek, A. Rowan, M. J. Crossley, R. J. M. Nolte, *J. Org. Chem.* **1999**, *64*, 6653.
- [17] H.-E. Fierz-David, L. Blangey, in *Grundlegende Operationen der Farbenchemie*, Springer-Verlag, Wien, 8th ed., **1952**, p. 244.
- [18] H. H. Hodgson, J. Walker, *J. Chem. Soc.* **1933**, 1620.
- [19] H. H. Hodgson, J. Walker, *J. Chem. Soc.* **1935**, 530.
- [20] R. Pütter, in: *Methoden der Organischen Chemie (Houben-Weyl)*, vol. X/3, p. 39, Thieme Verlag, Stuttgart, **1965**.
- [21] M. Erdélyi, A. Gogoll, *J. Org. Chem.* **2001**, *66*, 4165.
- [22] J. Eskildsen, T. K. Reenberg, J. B. Christensen, *Eur. J. Org. Chem.* **2000**, 1637.
- [23] P. Jacob, P. S. Callery, A. Shulgin, N. Castagnoli, *J. Org. Chem.* **1976**, *41*, 3627.
- [24] H. G. Viehe (Ed.), *Chemistry of Acetylenes*, Dekker, New York, **1962**.
- [25] F. Diederich, P. J. Stang, R. R. Tykwinski (Eds.), *Acetylene Chemistry*, Wiley-VCH, Weinheim, **2005**.
- [26] M. Pittelkow, T. I. Sølling, J. B. Christensen, *Org. Biomol. Chem.* **2005**, *3*, 2441.
- [27] A. Kapturkiewicz, *J. Electroanal. Chem.* **1986**, *201*, 205.
- [28] C. Rüssel, W. Jaenicke, *J. Electroanal. Chem.* **1984**, *180*, 205.
- [29] C. Rüssel, W. Jaenicke, *J. Electroanal. Chem.* **1986**, *200*, 249.
- [30] N. Gupta, H. Linschitz, *J. Am. Chem. Soc.* **1997**, *119*, 6384.
- [31] J. E. Heffner, C. T. Wigal, O. A. Moe, *Electroanalysis* **1997**, *9*, 629.
- [32] L. H. M. Janssen, A. L. van Til, F. B. van Duijneveldt, *Bioelectrochem. Bioenerg.* **1992**, *27*, 161.
- [33] M. E. Peover, *J. Chem. Soc.* **1962**, 4540.

- [34] C. Rüssel, W. Jaenicke, *J. Electroanal. Chem.* **1986**, *200*, 249.
- [35] A. Streitwieser Jr, *Molecular Orbital Theory for Organic Chemists*, Wiley, New York, **1961**, chapter 7.
- [36] O. G. Mekenyan, S. P. Bradbury, V. B. Kamenska, *SAR and QSAR in Environ. Res.* **1996**, *5*, 255.
- [37] M. E. Peover, *Nature* **1962**, *193*, 475.
- [38] S. Tsutsui, K. Sakamoto, H. Yoshida, A. Kunai, *J. Organomet. Chem.* **2005**, *690*, 1324.
- [39] P. Rapta, K. Erentova, A. Stasko, H. Hartmann, *Electrochim. Acta* **1994**, *39*, 2251.
- [40] X. Zhao, T. Kitagawa, *J. Raman Spectrosc.* **1998**, *29*, 773.
- [41] M. Aguilar-Martínez, J. A. Bautista-Martínez, N. Macías-Ruvalcaba, I. González, E. Tovar, T. Marín del Alizal, O. Collera, G. Cuevas, *J. Org. Chem.* **2001**, *66*, 8349.
- [42] M. E. Peover, in: *Electroanalytical Chemistry*, vol. 2 (Ed.: A. J. Bard) Dekker, New York, **1967**, p.1–51.
- [43] V. D. Parker, *J. Am. Chem. Soc.* **1976**, *98*, 98.
- [44] O. Hammerich, in: *Organic Electrochemistry*, 4th ed. (Eds.: O. Hammerich, H. Lund), Dekker, New York, **2001**, chapter 2.
- [45] D. S. Pedersen, C. Rosenbohm, *Synthesis* **2001**, *16*, 2431.
- [46] M. J. Frisch, G. W. Trucks, H. B. Schlegel, G. E. Scuseria, M. A. Robb, J. R. Cheeseman, J. A. Montgomery Jr, T. Vreven, K. N. Kudin, J. C. Burant, J. M. Millam, S. S. Iyengar, J. Tomasi, V. Barone, B. Mennucci, M. Cossi, G. Scalmani, N. Rega, G. A. Petersson, H. Nakatsuji, M. Hada, M. Ehara, K. Toyota, R. Fukuda, J. Hasegawa, M. Ishida, T. Nakajima, Y. Honda, O. Kitao, H. Nakai, M. Klene, X. Li, J. E. Knox, H. P. Hratchian, J. B. Cross, V. Bakken, C. Adamo, J. Jaramillo, R. Gomperts, R. E. Stratmann, O. Yazyev, A. J. Austin, R. Cammi, C. Pomelli, J. W. Ochterski, P. Y. Ayala, K. Morokuma, G. A. Voth, P. Salvador, J. J. Dannenberg, V. G. Zakrzewski, S. Dapprich, A. D. Daniels, M. C. Strain, O. Farkas, D. K. Malick, A. D. Rabuck, K. Raghavachari, J. B. Foresman, J. V. Ortiz, Q. Cui, A. G. Baboul, S. Clifford, J. Cioslowski, B. B. Stefanov, G. Liu, A. Liashenko, P. Piskorz, I. Komaromi, R. L. Martin, D. J. Fox, T. Keith, M. A. Al-Laham, C. Y. Peng, A. Nanayakkara, M. Challacombe, P. M. W. Gill, B. Johnson, W. Chen, M. W. Wong, C. Gonzalez, J. A. Pople, *Gaussian 03*, Revision C.02, Gaussian, Inc., Wallingford, CT, **2004**.
- [47] *GaussView 3.0*, Gaussian Inc., Carnegie Office Park, Building 6, Pittsburgh, PA 15106, USA; © Semichem, Inc., **2000–2003**.  
Received: February 1, 2006  
Published Online: ■

■ P. Hammershøj, T. K. Reenberg,  
M. Pittelkow, C. B. Nielsen, O. Hammerich,  
J. B. Christensen\*

 Synthesis and Properties of 2,3-Dialkynyl-1,4-benzoquinones

**Keywords:** Benzoquinones / Acetylenes / Sonogashira cross-coupling / Cyclic voltammetry / UV/Vis / DFT calculations

